

THERMAL DENATURATION OF GLOBULAR PROTEINS

Fourier Transform-Infrared Studies of the Amide III Spectral Region

GLORIA ANDERLE AND RICHARD MENDELSON

*Department of Chemistry, Newark College of Arts and Sciences, Rutgers University, Newark,
New Jersey 07102*

ABSTRACT Fourier transform-infrared (FT-IR) spectra are reported for the amide III spectral region of the native and thermally denatured forms of chymotrypsinogen, ribonuclease, bovine serum albumin, and lysozyme. Chymotrypsinogen denatures into structures containing substantial contributions from β -sheets, while lysozyme and bovine serum albumin show increased amounts of random-coil forms. The changes observed for ribonuclease are quite small.

Bovine serum albumin shows at least six bands in the 1,260–1,320 cm^{-1} region which undergo large intensity changes upon thermal denaturation, and hence are assignable to α -helical amide III modes. The large number of observed bands suggests that slight variations in helical geometry, symmetry, or interactions result in changed amide III frequencies, so that simple correlations between narrow frequency ranges and secondary structures may not be applicable for this mode. A widened frequency range is suggested as diagnostic for helical structures.

INTRODUCTION

The determination of protein secondary structure in solution remains an area of ongoing biophysical importance. Toward this end, vibrational spectroscopic techniques have been widely utilized (for reviews, see references 1–3). Two regions of the infrared spectrum, the amide I (peptide bond C=O stretch) and amide II (mixture of peptide bond C—N stretch and N—H inplane bend) have been most important in this context. In contrast, the amide III spectral region, although widely used in Raman spectroscopic investigations, has been comparatively neglected in IR work (see reference 4 for an exception to this) due to its relative weakness. Yet the vibration offers some advantages for IR study. The range of vibrational frequencies (1,230–1,300 cm^{-1}) observed for various secondary structures is somewhat greater than that for either amide I (1,630–1,685 cm^{-1}) or amide II (1,520–1,560 cm^{-1}). In addition, neither liquid water nor water vapor vibrations overlap with the amide III region, in contrast to the other modes. In particular, the subtraction of liquid water absorption in order to allow unhindered observation of the amide I spectral region remains a difficult task (5). Thus, estimation of secondary structure by use of the amide I mode has often required in practice the use of anhydrous material or replacement of H_2O by D_2O as solvent (6, 7). In the latter case, the resulting amide I' vibrations are slightly shifted in frequency (~ 3 –5 cm^{-1} lower than amide I) while the amide II modes are altered in position (to $\sim 1,450 \text{ cm}^{-1}$) so as to lie underneath the ever present HOD bending vibration.

In the current work, high quality FT-IR spectra have

been obtained for the amide III region of four globular proteins in aqueous solution in their native and thermally denatured states. The spectral alterations that occur upon thermal denaturation demonstrate the utility of, and difficulties with, this spectral region for IR studies of protein secondary structure.

MATERIALS AND METHODS

Materials

Proteins were obtained from Sigma Chemical Co. (St. Louis, MO), were of the highest quality available, and were used without further purification. They were dissolved in doubly distilled water at a concentration of 100 mg/ml, pH 7.0.

Methods

Samples were examined in a thermostatted transmission cell with CaF_2 windows and a path length of 50 μM . It is noted that reflectance cells were not required as H_2O absorption is minimal in the spectral region of interest in the current work. Cell temperatures were monitored with a thermocouple from Sensortek, Inc. (Clifton, NJ) placed close to the cell windows but out of the optical path. FT-IR data were acquired with a Sirius 100 spectrophotometer from Mattson Instruments (Madison, WI). Routinely, 1,000 interferograms were acquired, co-added, apodized with a triangular function, and Fourier transformed to yield a spectrum with 4 cm^{-1} resolution. One level of zero filling resulted in data encoded every 2 cm^{-1} . The sample chamber was purged with dried N_2 gas. Data were baseline leveled between 1,215 and 1,365 cm^{-1} .

RESULTS AND DISCUSSION

Spectra for the 1,220–1,360 cm^{-1} region of native and thermally denatured chymotrypsinogen, native α -chymotrypsin, ribonuclease, bovine serum albumin, and lysozyme

are shown in Figs. 1–5, respectively, while the observed frequencies are tabulated in Tables I–IV. Included for comparative purposes in Tables I–IV are Raman spectral data for the amide III spectral region as reported in various studies by other groups. Estimates of protein secondary structures as derived either from x-ray crystallography or spectroscopic methods are given in Table V. Thermal denaturation of each protein produces substantial alterations in the amide III band contours as discussed below.

Chymotrypsinogen

Chymotrypsinogen (Fig. 1 and Table I) in its native form reveals amide III vibrations at 1,237, 1,250, 1,256, and 1,281 cm^{-1} . The lowest frequency vibration is assigned to the β -sheet conformation while the mode at 1,281 cm^{-1} is appropriate for the α helix. Thermal denaturation produces extensive changes in the amide III spectral region. The band at 1,281 cm^{-1} is reduced in intensity, indicative of loss of α -helical structure (8). The 1,250 band and 1,256 shoulder are also reduced in intensity, while the band at 1,237 cm^{-1} shows a substantial intensity increase as well as a small (2 cm^{-1}) frequency reduction. As this frequency position is appropriate for β -structure, it is concluded that chymotrypsin denatures into structures possessing the β type of H-bonding and appropriate inter- and intrachain vibrational coupling.

The amide III regions of chymotrypsinogen and α -chymotrypsin are compared in Fig. 2. Differences are noted which suggest that the removal of residues 1–15 and

TABLE I
FTIR AND RAMAN FREQUENCIES* AND RELATIVE INTENSITIES OF AQUEOUS CHYMOTRYPSINOGEN AND α -CHYMOTRYPSIN IN THE 1,360–1,220 cm^{-1} REGION

Chymotrypsinogen				α -Chymotrypsin			
FTIR				FTIR (Native)		Raman‡	
Native		Denatured		3.4°C		(Native)	
4.9°C		83.9°C				25°C	
1,343	(4)	1,352	(0)			1,361	(3)
1,336 sh	(3)	1,343	(1)	1,343	(3)	1,340	(7)
1,333 sh	(2)	1,337	(1)	1,339 sh	(2)		
1,319	(2)	1,323	(0)			1,321	(1)
1,316 sh	(2)	1,316	(1)	1,316	(1)		
1,310	(1)	1,310	(1)			1,300	(0)
		1,302 sh		1,300 sh			
		1,289 sh					
1,281	(7)	1,279	(5)	1,279 sh	(5)		
		1,264 sh		1,264 sh	(9)	1,268 sh	(3)
1,256 sh		1,256 sh		1,256	(10)		
1,250	(10)			1,250	(10)		
		1,246 sh	(7)			1,246	(9)
		1,240 sh	(9)				
1,237	(8)	1,235	(10)	1,237 sh	(7)		
		1,227 sh	(10)				

*sh denotes shoulder.

‡Reference 20.

TABLE II
FTIR AND RAMAN FREQUENCIES* AND RELATIVE INTENSITIES OF AQUEOUS RIBONUCLEASE-A IN THE 1,360–1,220 cm^{-1} REGION

FTIR		Raman‡	
Native	Denatured	Native	Denatured
1.2°C	71.3°C	32°C	70°C
1,358 sh (1)			
1,348 (2)	1,352 sh (1)		
1,343 (2)	1,345 (1)		
1,335 (2)	1,337 (1)	1,337 (3)	1,337 sh (3)
	1,331 (1)		
1,325 sh	1,323 (1)	1,324 sh (1)	1,320 (8)
1,316 (4)	1,317 (1)	1,315 (8)	
1,312 sh (3)	1,310 sh (1)		
	1,302 sh (1)		
1,296 sh (3)	1,290 sh (1)		1,290 sh (0)
1,285 sh (4)	1,279 sh (2)	1,284 sh (0)	
1,262 sh (5)	1,260 sh (8)	1,263 (10)	1,260 (11)
1,257 sh (8)	1,254 sh (9)		
1,250 sh (9)	1,248 (10)		
1,242 (10)	1,240 sh (10)	1,239 (11)	1,242 (11)
1,237 sh (9)			

*sh denotes a shoulder.

‡Reference 9.

247–249 (which takes place upon conversion of chymotrypsinogen to α -chymotrypsin) induces substantial changes in the secondary structure of the molecule. The peak at 1,281 cm^{-1} is reduced in intensity, indicating loss of helical structure. The helix content for both molecules as predicted from various methods is summarized in Table V.

TABLE III
FTIR AND RAMAN FREQUENCIES* AND RELATIVE INTENSITIES OF AQUEOUS BOVINE SERUM ALBUMIN IN THE 1,360–1,220 cm^{-1} REGION

FTIR		Raman		
Native	Denatured	Solid‡	Native	
1.2°C	74.8°C		25°C‡	25°C§
1,368 (1)				
1,360 sh (1)	1,362 (1)			
1,352 sh (1)	1,350 sh (0)			
1,343 (3)	1,346 sh (1)			
1,335 sh (4)	1,340 (1)	1,337	1,337	1,337 (8)
1,319 sh (8)	1,316 (3)	1,320	1,317	1,317 (7)
1,312 (9)				
1,300 (10)				
1,294 sh (10)	1,296 (4)			
1,285 sh (9)	1,281 sh (8)	1,278		1,280 sh (6)
1,269 (8)			1,268	
1,264 sh (8)	1,264 (10)			
1,250 (8)	1,250 sh (9)		1,252	1,250 (4)
		1,246		

*sh denotes shoulder.

‡Reference 14.

§Reference 13.

TABLE IV
FTIR AND RAMAN FREQUENCIES* AND RELATIVE
INTENSITIES OF AQUEOUS LYSOZYME IN THE
1,360–1,220 cm^{-1} REGION

FTIR		Raman†	
Native 1.6°C	Denatured 71.6°C	Native 25°C	Denatured 80°C
1,354 sh (2)			
1,343 (5)	1,342 (4)		1,341 (7)
1,335 sh (2)	1,337 (4)	1,337 (7)	
1,321 sh (4)	1,320 (4)		
1,316 (5)		1,313 (0)	1,313 (0)
	1,310 sh (3)		1,306 (2)
1,298 (5)	1,298 sh (6)	1,300 (1)	
1,289 (6)		1,288 (0)	1,288 (0)
1,279 sh (8)	1,281 sh		
	1,275 sh	1,272 sh (0)	1,272 sh (0)
1,264 (10)	1,264 sh (10)		
1,256 sh (10)	1,258 (10)	1,258 (5)	1,256 (6)
	1,250 sh (10)		
1,238 sh (7)	1,237 sh (8)	1,239 (1)	1,239 (1)

*sh denotes a shoulder.

†Reference 19.

The variation for each molecule from technique to technique is not unexpected, as each experimental approach uses a different standard for what constitutes an α -helix. We note, however, that for each individual type of experiment, a reduction of helix content (albeit very slight, and possibly insignificant) is observed upon chymotrypsin formation. Further changes are observed in the amide III region when chymotrypsin is formed. A new intense shoulder at $1,263 \text{ cm}^{-1}$ (partially resolved from the $1,256 \text{ cm}^{-1}$ band) is evident in the α -chymotrypsin spectrum. This may result from helical segments that differ in flexibility and interactions from those giving rise to the $1,281 \text{ cm}^{-1}$ band in chymotrypsinogen. Some loss of

TABLE V
SECONDARY STRUCTURE OF PROTEINS USED IN THE
CURRENT STUDY

Protein	α -Helix	β -Structure	Other	Reference
	%	%	%	
α -Chymotrypsin	12	51	37	17
	10	49	41	16
	8	22	70	21
	15	29	56	22
Chymotrypsinogen	13	49	38	17
	11	46	43	16
	20	20	60	21
Ribonuclease-A	21	50	29	17
	22	46	21	16
	12	36	52	21
	25	44	31	22
Bovine serum albumin	55	0	45	11
Lysozyme	41	21	38	17
	45	19	36	16
	35	10	55	21

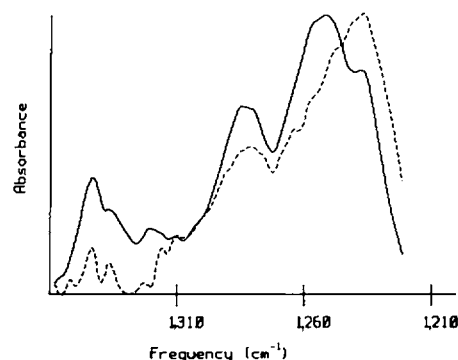


FIGURE 1 FTIR amide III region of native (solid line) and thermally denatured (dashed line) chymotrypsinogen in H_2O at pH 7. The path-length was $50 \mu\text{M}$ and windows were CaF_2 . The spectra were baseline leveled from $1,365$ to $1,215 \text{ cm}^{-1}$.

β -structure (as marked by the reduction of the shoulder near $1,236 \text{ cm}^{-1}$) is also apparent.

Ribonuclease

Ribonuclease possesses a secondary structure distribution similar to that found in chymotrypsinogen, with α -helical contents of 12–25% and β -sheet contents of between 36 and 50% having been reported (Table V). Chen and Lord (9) have investigated changes in the amide III region of the Raman spectrum that occur upon thermal denaturation of this molecule. In the native enzyme, they observed two poorly resolved features at $1,239$ and $1,260 \text{ cm}^{-1}$ along with a shoulder at $1,284 \text{ cm}^{-1}$. Thermal denaturation of the enzyme produced a spectrum with two peaks ($1,242$ and $1,260 \text{ cm}^{-1}$) better resolved than in the native structure. In the current FT-IR data (Fig. 3 and Table I) spectral patterns in the amide III region differ substantially from those observed in the Raman experiments. The main feature in the native enzyme is a peak at $1,242 \text{ cm}^{-1}$. This is accompanied by a series of shoulders at $1,237$, $1,250$, $1,257$, and $1,262 \text{ cm}^{-1}$. Thermal denaturation causes small shifts in the intensity distribution around this

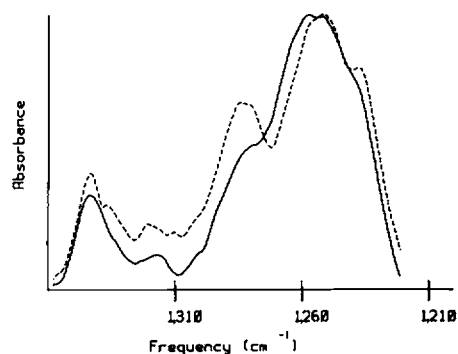


FIGURE 2 FTIR amide III region of native (solid line) chymotrypsinogen and native (dashed line) α -chymotrypsin in H_2O at pH 7. Pathlength was $50 \mu\text{M}$ and windows were CaF_2 . The spectra were baseline leveled from $1,365$ to $1,215 \text{ cm}^{-1}$.

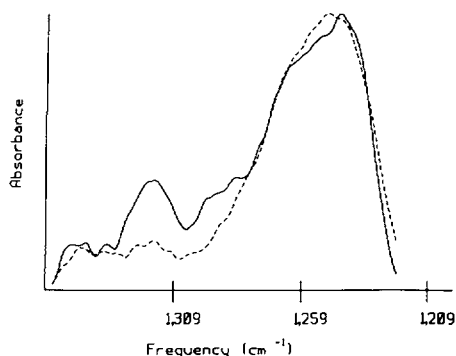


FIGURE 3 FTIR amide III region of native (solid line) and thermally denatured (dashed line) ribonuclease-A in H₂O at pH 7. The pathlength was 50 μ M and windows were CaF₂. The spectra were baseline leveled from 1,365 to 1,215 cm^{-1} .

band, so that the resultant contour has a maximum at 1,248 cm^{-1} .

The above data suggest that the feature near 1,242 cm^{-1} and shoulder at 1,237 be assigned to β -sheet structure, partial loss of which occurs upon thermal denaturation. The resultant intensity increase near 1,248 cm^{-1} arises from irregular conformations.

Differences between the observed amide III contours as observed by FT-IR and Raman spectroscopy can be traced to the following three factors: first, the different intensities of side-chain modes will complicate the amide III spectral contours to different extents in IR and Raman spectroscopy. Second, the presence of relatively extensive segments of a particular secondary structure (particularly in native ribonuclease) results in a symmetry-based splitting of a particular vibrational band. The resultant components of the peak may have different IR and Raman activities. Finally, for low symmetry structures, there will be different inherent relative intensities in IR and Raman spectroscopy.

It is evident (compare Figs. 1 and 3) that thermal denaturation of ribonuclease produces conformations substantially different from those induced in chymotrypsinogen. In the former, the production of random-coil structures is apparent, while in the latter the appearance of β -sheet bands in the spectrum suggests the widespread occurrence of intermolecular aggregation resulting in a shift in the distribution of β -sheet structures.

Finally, although the α -helical content of ribonuclease is probably higher than that for chymotrypsinogen, the only spectral feature immediately assignable to that secondary structure is the shoulder at 1,262 cm^{-1} . It is therefore tempting to assign the band at 1,316 cm^{-1} (which is substantially reduced in intensity on thermal denaturation) to the helical structure, although we recognize that the frequency falls outside the range commonly cited for α -helical amide III (8, 10). However, evidence for high frequency ($>1,300 \text{ cm}^{-1}$) α -helical amide III modes in bovine serum albumin is presented below, and their postulated occurrence in ribonuclease is reasonable.

Bovine Serum Albumin

Evidence for high frequency α -helical amide III vibrations comes from spectra of bovine serum albumin (Fig. 4). The helical content for the native protein is estimated at 55% (11) (Table V). The protein is thought to possess little or no β -sheet structure. Spectra of the native material show intense bands or shoulders at 1,319, 1,312, 1,300, 1,294, and 1,285 cm^{-1} , all of which are markedly reduced in intensity upon thermal denaturation. Since it is unlikely that side-chain vibrations would be altered in such fashion, the series of bands must be assigned (at least for the most part) to protein peptide bond amide III modes. The wide variety of bands is, as suggested by Hsu et al. (12), inconsistent with the assignment of a narrow range of frequencies to a particular secondary structure.

In addition to the high frequency features arising from helical domains, other bands are apparent at 1,250, 1,264, and 1,269 cm^{-1} . The lowest of these probably arises from irregular conformations, the others probably from additional helical segments. Thermal denaturation produces additional random-coil structures (1,250 cm^{-1}), yet substantial helical domains remain (1,260–1,285 cm^{-1}). These have frequencies that differ from the native molecule and reflect possible changes in the nature of the helix or in the interactions between domains of helices.

There are profound differences between the amide III region in the current FT-IR data and the Raman studies of Bellocq et al. (13) and Lin and Koenig (14). The Raman bands arising from helical amide III modes are extremely weak, to the point of being difficult to detect, whereas the random coil amide III vibrations are relatively more intense in the Raman spectra than in the FT-IR. Side-chain modes arising in part from Trp tend to complicate the 1,300–1,350 cm^{-1} region of the Raman spectrum.

Lysozyme

The final protein studied in the current work is lysozyme. Secondary structure changes induced by a variety of agents have been extensively probed by Lord and co-workers (15)

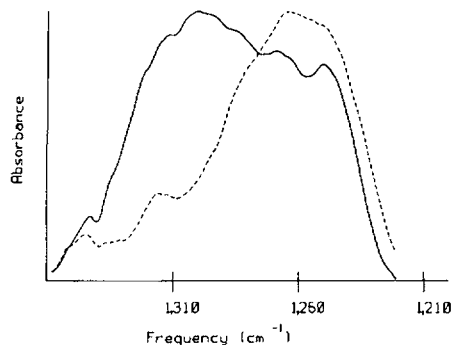


FIGURE 4 FTIR amide III region of native (solid line) and thermally denatured (dashed line) bovine serum albumin in H₂O at pH 7. The pathlength was 50 μ M and windows were CaF₂. The spectra were baseline leveled from 1,365 to 1,215 cm^{-1} .

using Raman spectroscopy. X-ray diffraction results (16) suggest 45% α -helix, 19% β -sheet, and 36% irregular structure, while spectroscopic methods yield values close to these (Table V). The FT-IR data (Fig. 5) show small changes in the intensity distribution of the amide III mode during thermal denaturation. The series of bands peaking around $1,264\text{ cm}^{-1}$ in the native enzyme seem to have their frequencies, at most, slightly altered upon denaturation, but the position of maximum intensity is lowered to $1,258\text{ cm}^{-1}$, due to a change in the distribution of intensities in the various components. This is consistent with the formation of an additional percentage of irregular structure upon irreversible denaturation, as had been deduced from Raman spectroscopic data (15). Consistent with this observation is the intensity decrease of a band and two shoulders centered near $1,315\text{ cm}^{-1}$.

CONCLUSIONS

The observation of numerous bands in the amide III spectral region is consistent with the suggestion of Byler and Susi (17) (who used amide I data) that simple correlations of particular frequencies with helical secondary structures is an oversimplification. The data for bovine serum albumin best exemplify this. There are at least seven spectral features in the region $1,260\text{--}1,320\text{ cm}^{-1}$ which are in the range appropriate for helical structures and which are dramatically weakened upon thermal denaturation.

The observation of so many amide III helical modes may be the result of several factors. The short length of helical segments coupled with variations in side chains may cause deviations from ideal geometry as well as alterations in vibrational coupling between peptide bonds due to loss of idealized symmetry. Dwivedi and Krimm (18) have shown that slight changes in geometry upon going from the α I to the α II helix produce substantial spectral shifts in the peptide bond modes. Changed interaction between domains may also contribute to altered IR frequency patterns.

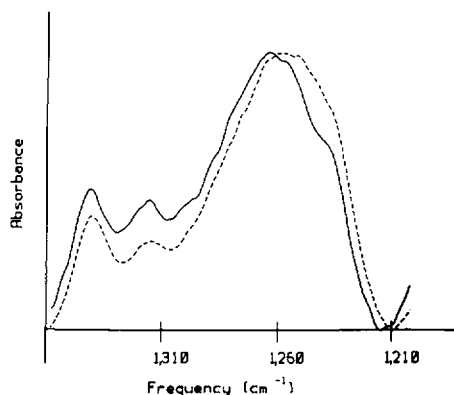


FIGURE 5 FTIR Amide III region of native (solid line) and thermally denatured (dashed line) lysozyme in H_2O at pH 7. The pathlength was $50\text{ }\mu\text{m}$ and windows were CaF_2 . The spectra were baseline leveled from $1,365$ to $1,215\text{ cm}^{-1}$.

What is the overall utility of the amide III frequency in the IR spectrum for studies of protein secondary structure? Unlike the amide I vibration, which occurs at about the same frequency ($1,650\text{--}1,660\text{ cm}^{-1}$) for α -helical and random-coil structures, the amide III vibration is clearly able to distinguish between these two classes of secondary structure. The following frequency ranges are considered the best available at present for the correlation of amide III modes with secondary structure: $1,315\text{--}1,260\text{ cm}^{-1}$, α or other forms of helix; $1,255\text{--}1,245\text{ cm}^{-1}$, irregular structure; and $1,242\text{--}1,230\text{ cm}^{-1}$, β -structure. In addition, the intensity of the helical components in the IR spectrum is strong compared with Raman spectroscopy (compare Fig. 3 in the current work with the Raman study of Lin and Koenig [14]). Finally, observation of the amide III region in the IR does not require either subtraction of water or use of D_2O as solvent such as is needed for the amide I. Although the amide III mode is $\sim 5\text{--}10$ -fold weaker than the amide I in the IR, it is detectable in a straightforward fashion with modern instrumentation.

Support was provided for this work through a National Institutes of Health grant (GM-29864) to Dr. Richard Mendelsohn.

Received for publication 22 September 1986 and in final form 10 February 1987.

REFERENCES

1. Lord, R. C., and N. T. Yu. 1970. Laser excited Raman spectroscopy of biomolecules. I. Native lysozyme and its constituent amino acids. *J. Mol. Biol.* 50:509-524.
2. Carey, P. R. 1982. *Biochemical Applications of Raman and Resonance Raman Spectroscopy*. Academic Press, Inc., New York. 71-98.
3. Fringeli, U. P., and Hs. H. Gunthard. 1980. Infrared membrane spectroscopy. *Mol. Biol. Biochem. Biophys.* 31:270-332.
4. Smith, K. B., C. A. Penkowski, and R. J. Jakobsen. 1985. Determination of protein structure by FTIR. Proceedings of the 1985 International Conference on Fourier and Computerized Infrared Spectroscopy. J. C. Grasselli and D. G. Cameron, editors. SPIE-International Society for Optical Engineering. 553:178.
5. Therrien, M., M. Lafleur, and M. Pezolet. 1985. On the water subtraction in the Fourier Transform Infrared (FTIR) spectra of proteins and lipids. Proceedings of the 1985 International Conference on Fourier and Computerized Infrared Spectroscopy. J. C. Grasselli and D. G. Cameron, editors. SPIE-International Society for Optical Engineering. 553:173-174.
6. Chirgadze, Y. N., B. V. Shestopalov, and S. Y. Venyaminov. 1973. Intensities and other spectra parameters of infrared amide bands of polypeptides in the β - and random forms. *Biopolymers*. 12:1337-1351.
7. Rothschild, K. J., and N. A. Clark. 1979. Anomalous amide I infrared absorption of purple membrane. *Science (Wash. DC)*. 204:311-312.
8. Yu, M. T., C. S. Liu, and D. C. O'Shea. 1972. Laser Raman spectroscopy and the conformation of insulin and proinsulin. *J. Mol. Biol.* 70:117-132.
9. Chen, M. C., and R. C. Lord. 1976. Laser Raman spectroscopic studies of the thermal unfolding of ribonuclease A. *Biochemistry*. 15:1889-1897.
10. Koenig, J. L., and B. Frushour. 1972. Raman studies of the helix-to-coil transition in poly-L-glutamic acid and poly-L-ornithine. *Biopolymers*. 11:1871-1892.

11. Schechter, E., and E. R. Blout. 1964. An analysis of the optical rotatory dispersion of polypeptides and proteins. *Proc. Natl. Acad. Sci. USA*. 51:695-702.
12. Hsu, S. L., W. H. Moore, and S. Krimm. 1976. Vibrational spectrum of the unordered polypeptide chain: a Raman study of feather keratin. *Biopolymers*. 15:1513-1528.
13. Bellocq, A. M., R. C. Lord, and R. Mendelsohn. 1972. Laser-excited Raman spectroscopy of biomolecules. III. Native bovine serum albumin and β -lactoglobulin. *Biochim. Biophys. Acta*. 257:280-287.
14. Lin, V. J. C., and J. L. Koenig. 1976. Raman studies of bovine serum albumin. *Biopolymers*. 15:203-221.
15. Chen, M. C., R. C. Lord, and R. Mendelsohn. 1974. Laser-excited Raman spectroscopy of biomolecules. V. Conformational changes associated with the chemical denaturation of lysozyme. *J. Am. Chem. Soc.* 96:3038-3042.
16. Levitt, M., and J. Greer. 1977. Automatic identification of secondary structure in globular proteins. *J. Mol. Biol.* 114:181-239.
17. Byler, M. D., and H. Susi. 1986. Examination of the secondary structure of proteins by deconvoluted FTIR spectra. *Biopolymers*. 25:469-487.
18. Dwivedi, A. M., and S. Krimm. 1984. Vibrational analysis of peptides, polypeptides, and proteins. XVIII. Conformational sensitivity of the α -helix spectrum: α_1 - and α_{11} -poly(L-alanine). *Biopolymers*. 23:923-943.
19. Brunner, H., and H. Sussner. 1972. Raman scattering of native and thermally denatured lysozyme. *Biochim. Biophys. Acta*. 271:16-22.
20. Chen, M. C., and R. C. Lord. 1980. Laser excited Raman spectroscopy of biomolecules. 13. Conformational study of α -chymotrypsin and trypsin. *J. Raman Spectrosc.* 9:304-307.
21. Saxena, V. P., and D. B. Wetlaufer. 1971. A new basis for interpreting the circular dichroic spectra of proteins. *Proc. Natl. Acad. Sci. USA*. 68:969-972.
22. Chou, P. Y., and G. D. Frasman. 1974. Prediction of protein structure. *Biochemistry*. 13:222-245.